Epitaxial nanowires

Evolution of Epitaxial InAs Nanowires on GaAs (111)B**

Xin Zhang, Jin Zou, Mohanchand Paladugu, Yanan Guo, Yong Wang, Yong Kim, Hannah J. Joyce, Qiang Gao, H. Hoe Tan, and Chennupati Jagadish*

Epitaxial III–V semiconductor nanowires (NWs) have attracted considerable attention due to their potential applications in nanoelectronics and optoelectronics.[1] Through the vapour–liquid–solid mechanism[2] the growth of III–V NWs has been successfully realized.[3] Nevertheless, the evolution of epitaxial NWs is poorly understood so far although such knowledge is vital for designing and manufacturing future NW devices. In this Communication, we present a systematic investigation of the Au catalyst-assisted growth of epitaxial InAs NWs on GaAs$\{111\}_B$ substrates. We find that the Au catalysts preferentially retain contact with GaAs, leading to the formation of horizontal InAs traces on the GaAs substrate in the initial growth stage. Vertical InAs NWs initiate at points where elongated traces intersect. This novel NW evolution phenomenon is attributed to the interfacial energy between the catalyst and InAs being higher than that between the catalyst and GaAs.

The unique physical characteristics of InAs[4] have made it an ideal electron-confinement material in quantum wells,[5] quantum dots,[6] and NW heterostructures.[7] For this reason, InAs NWs are predicted to be of great future importance and are chosen as the subject of this study. In fact, considerable effort has been devoted to InAs NW growth from as early as the 1990s.[8] It has been found that, unlike their quantum-well and quantum-dots counterparts,[5,6] epitaxial InAs NWs are preferentially grown in the form of the wurtzite (WZ) structure.[9] As a consequence, when grown on the zinc blende (ZB)-structured GaAs or InAs $\{111\}_B$ substrates, InAs NWs tend to grow along the $[000\bar{1}]$ direction.[8,10] Nevertheless, ZB-structured InAs NWs with [110] and [100] growth direction fabricated by reacting In with GaAs $(111)_B$ substrate[11] or NWs with <111> direction synthesized by annealing $\{111\}_B$ InAs wafer covered by Au[12] were also demonstrated. Although InAs NWs have been studied extensively, the initiation of NW growth remains unclear, especially for the heteroepitaxial systems. In this study, InAs NWs were grown on GaAs $\{111\}_B$ substrates by MOCVD (for details see Experimental Section) for different durations, namely 1, 5, 10, and 60 min. The large lattice mismatch (7.2%) between GaAs and InAs and interfacial energy could significantly influence NW nucleation and growth.

Figure 1 shows typical scanning electron microscopy (SEM) images of InAs NWs with different growth times. No vertical NWs were found in the sample with 1 min growth of InAs (Figure 1a). Instead, short traces, lying on the substrate, can be seen with Au catalysts at one end of each trace (arrowed in the inset). With 5 min growth of InAs

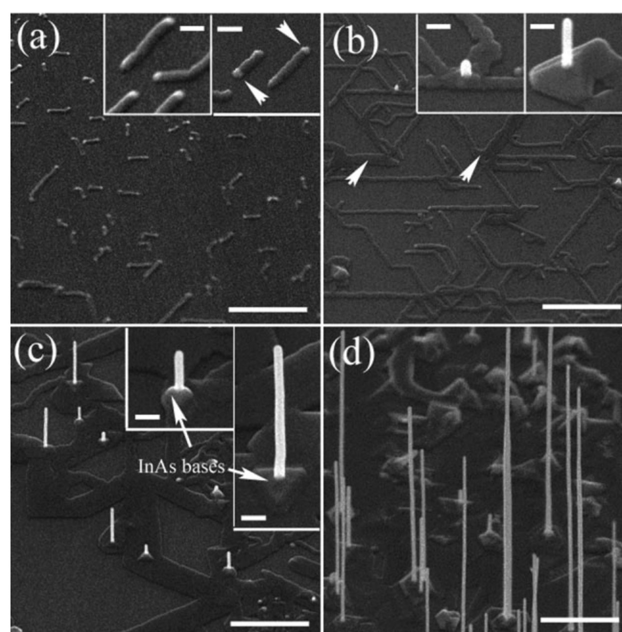

Figure 1. The general morphology of the samples at different growth stages (substrates tilted to 45°) of a) 1 min, b) 5 min, c) 10 min, and d) 60 min. The insets show the details of surface structure and NWs. The scale bars = 1 μm (100 nm for the insets).

[*] Prof. J. Zou, Dr. X. Zhang,+ M. Paladugu, Y.-N. Guo, Dr. Y. Wang
School of Engineering
The University of Queensland
Brisbane, QLD 4072 (Australia)
E-mail: j.zou@uq.edu.au

Prof. J. Zou
Centre for Microscopy and Microanalysis
The University of Queensland
Brisbane, QLD 4072 (Australia)

Prof. Y. Kim
Department of Physics
Dong-A University
Hadan-2-dong, Sahagu, Busan (Korea)

H. J. Joyce, Dr. Q. Gao, Dr. H. H. Tan, Prof. C. Jagadish
Department of Electronic Materials Engineering
Research School of Physical Sciences and Engineering
The Australian National University
Canberra ACT 0200 (Australia)

[+] On leave from the Department of Material Science
Fudan University
Shanghai 200433 (P.R. China)

[**] This research is supported by the Australian Research Council.

DOI: 10.1002/smll.200800690

 WILEY InterScience DISCOVER SOMETHING GREAT

© 2009 Wiley-VCH Verlag GmbH & Co. KGaA, Weinheim

(Figure 1b), the traces elongate with most of them forming a network. Two characteristics can be noted from Figure 1b: 1) the initiation of vertical NWs on the traces is observed occasionally (shown in the inset) and 2) some traces become wider (as indicated by arrows). Increasing the InAs growth to 10 min (Figure 1c), networked traces are observed. In this sample, a number of vertical free-standing NWs with various heights are observed emerging out on the traces with each NW having a triangle foundation structure at its base in addition to the trace. It is of interest to note that traces have widened when compared with those in the sample with 5 min growth of InAs, suggesting that the trace widening takes place when traces are blocked for their elongation on the GaAs surface. When the InAs growth is increased to 60 min (Figure 1d), no traces are seen. Instead, many vertical NWs with various heights (from tens of nm to several μm) are observed. Comparing Figure 1c with d, we deduce that the disappearance of traces in the latter case indicates that the widened traces have merged to cover the entire GaAs substrate.

An interesting phenomenon is that the traces in samples with shorter growth time ($\leq$10 min) elongate in specific crystallographic directions, as shown in the on-zone SEM image (Figure 2a where the electron beam is parallel to the substrate normal), that is, traces form equilateral triangular shapes. The only two possible families of equivalent crystallographic directions that are on GaAs $\{111\}_B$ plane with each having three individual orientations (note that $[uvw]$ is antiparallel to $[\overline{uvw}]$; the six $\langle uvw \rangle$ directions on the GaAs surface lead to three $\langle uvw \rangle$ orientations) with 60° between them are $\langle 110 \rangle$ and $\langle 112 \rangle$, as schematically illustrated in Figure 2b.

To understand the formation mechanism of these traces, extensive $\langle 110 \rangle$ cross-sectional transmission electron microscopy (TEM) investigations were carried out on the sample with 5 min growth of InAs. In Figure 2c, cross sections of short traces can be seen whereas, in Figure 2d, part of a long trace with a *head* at the end of the trace is seen. By comparing the side view of traces in Figure 2c and d (view along a $\langle 110 \rangle$ direction) with those viewed from the top (Figure 2a, viewed along the [111] direction), we conclude that the traces elongate along the $\langle 112 \rangle$ directions. Energy-dispersive X-ray spectroscopy (EDS) analysis (not shown here) confirmed that the traces are pure InAs, and the *head* shown in Figure 2d is a Au-dominated Au–In alloy. Since there exists a 7.2% difference in the lattice parameters between InAs ($a_{InAs} = 0.606$ nm) and GaAs ($a_{GaAs} = 0.565$ nm), InAs traces could be strained by the substrate and the role of strain in the trace formation must be examined. High-resolution (HR) TEM investigations were performed at the trace/substrate interface to determine the strain status. An example is shown in Figure 2e, where many misfit dislocations (indicated by arrows) can be clearly observed at the InAs/GaAs interface. Figure 2f is the optical diffractogram (OD, equivalent to the electron diffraction) pattern taken from the interface region shown in Figure 2e and shows clearly the splits of two {111}* reflections with the inner one being InAs (due to its larger lattice parameter) and the outer one being GaAs. Both the HRTEM image and the OD pattern also illustrate that InAs and GaAs have the ZB structure. Careful measurement of the two sets of diffraction

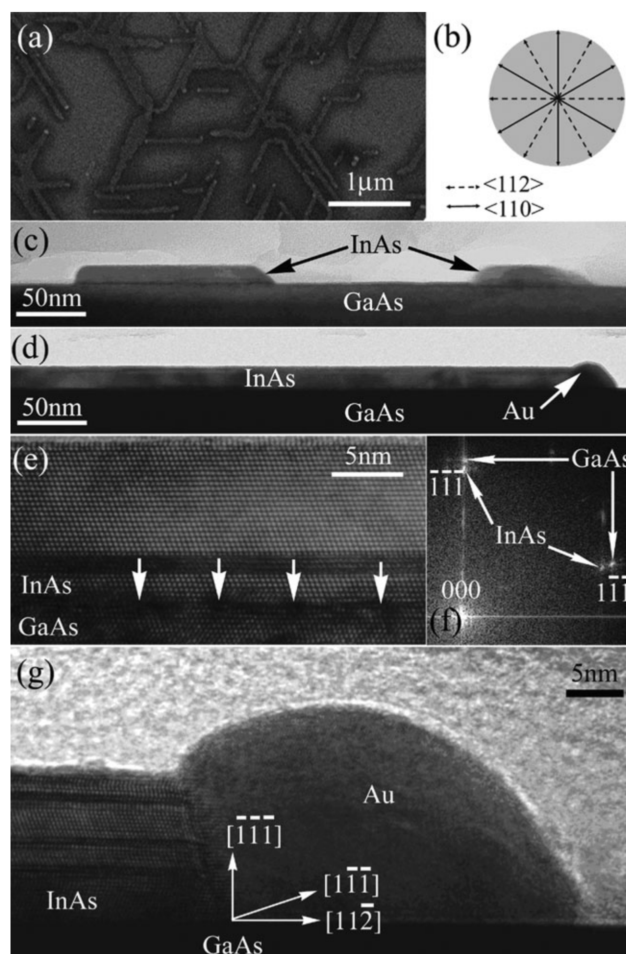

Figure 2. a) On-zone SEM image illustrating the trace orientation taken from the sample with 5 min growth of InAs; b) sketch of the orientational relationship between ⟨110⟩ and ⟨112⟩ directions on a (111) plane; c,d) general morphologies of the traces taken from ⟨110⟩ XTEM specimens; e) HRTEM image from the InAs/GaAs interface region showing the atomic structure with misfit dislocations; f) part of an OD pattern from which the lattice mismatch can be determined; g) intersection structure of the catalyst, InAs trace, and GaAs substrate showing that the catalyst retains an interface with InAs {111}.

patterns indicates a difference of lattice parameters of $7.0 \pm 0.5\%$. Thus, the lattice mismatch between InAs and GaAs substrate has been almost relaxed through the formation of misfit dislocations at the interface during the trace formation. This result suggests that the system does not increase the strain energy during the trace formation, so that the lattice mismatch only plays a minor or no role in trace formation.

To understand trace formation we note that, in our recent study of InAs/GaAs NW heterostructures, the interfacial energy of InAs/Au is higher than that of GaAs/Au, and these energetic considerations resulted in the Au catalysts retaining contact with GaAs.[13] In this study, the Au catalyst also tends to retain contact with the GaAs substrate; we believe that this is also due to the low Au–GaAs interfacial energy, leading to the catalysts minimizing contact with InAs. Therefore, with further supply of In and As vapors, the Au catalyst moves horizontally on the GaAs substrate to minimize system energy, leading to the trace formation and elongation.

© 2009 Wiley-VCH Verlag GmbH & Co. KGaA, Weinheim

To answer the question why traces elongate along the ⟨112⟩ directions, HRTEM investigations were carried out around the catalysts. Figure 2g shows such an example, where the interfaces of Au–InAs (the traces) and Au–GaAs (the substrate) can be found to be all in {111} crystallographic planes for InAs and GaAs, which suggests that the {111} interfacial energies between the catalyst and InAs/GaAs are relatively smaller than that of other crystallographic planes. Our extensive observations suggest that the trace formation must be led by the movement of the liquid catalysts; the moving catalyst prefers to retain an InAs {111} interface during the trace elongation and the angle between the Au/InAs {111} interface and the Au/GaAs $\{111\}_B$ interface is always an obtuse angle. Based on this, the catalysts must then move along directions that are perpendicular to the intersection of the GaAs $\{111\}_B$ plane (the GaAs surface) and the catalyst/InAs interfaces (other {111} planes). Crystallographically speaking, 1) the intersections of two non-parallel {111} atomic planes must be parallel to the ⟨110⟩ orientations and 2) within the GaAs surface being $\{111\}_B$, those directions that are perpendicular to the ⟨110⟩ orientations must be the ⟨112⟩ directions (refer to Figure 2b). As a consequence, traces must elongate along the ⟨112⟩ directions. It should be noted that, as shown in Figure 2b, there are six ⟨112⟩ directions within the GaAs surface and we have observed traces moving along all six ⟨112⟩ directions. Since the direction of any [*uvw*] is anti-parallel to that of $[\overline{uvw}]$, the six ⟨112⟩ directions on the GaAs surface lead to three ⟨112⟩ orientations (as shown in Figure 2b), so that the trace network in the form of equalized triangles is observed.

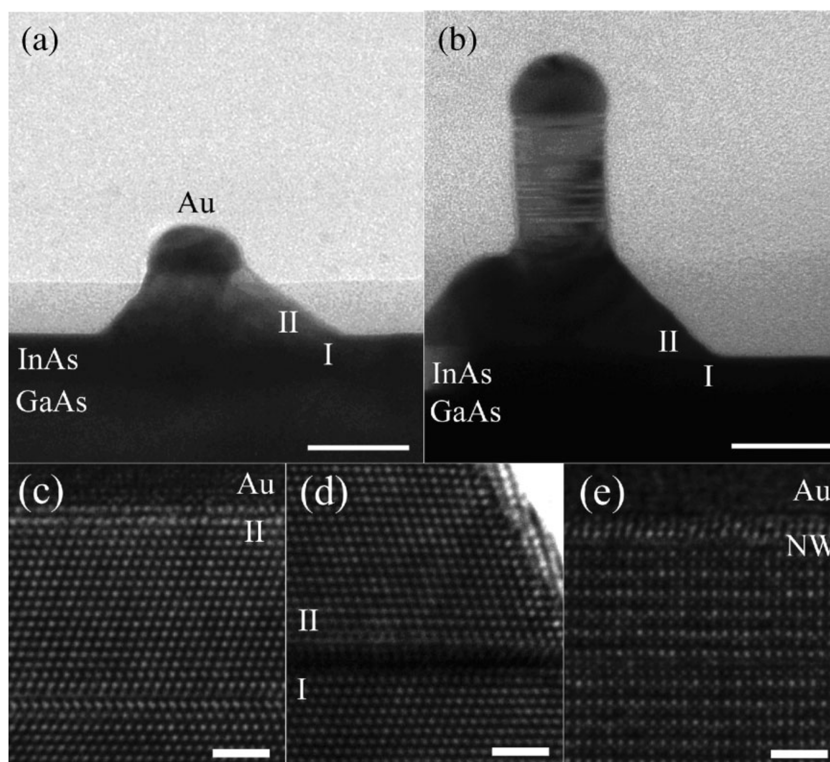

Figure 3. a) Bright-field image taken from Au particle with its underlying base. b) Developed NW with the underlying structures. c) HRTEM image showing the interface structure between Au and ZB-structured base in (a); d) interface structure between InAs trace (I) and base (II), and (e) HRTEM image of the area just under the Au particle shown in (b), showing the wurtzite structure of the developed InAs NW. Scale bars of (a) and (b) are 50 nm, (c–e) are 2 nm.

It is of interest to note that vertical NWs initiate at trace intersections where the Au catalysts can no longer retain interfaces with the GaAs substrate. Similar phenomena have been observed in growing branched InAs NWs around GaAs NW stems.[14] Figure 3a and b shows two typical cross-sectional TEM images, before and after the initiation of vertical InAs NWs performed in samples with 10 and 60 min of InAs growth. Consistent with the SEM observation, bases (marked as II) are always found in our vertical NWs (including those just about to be developed, as shown in Figure 3a). HRTEM investigations confirmed that the surfaces (under the bases) shown in Figure 3a and b are InAs, similar to that shown in Figure 2e, even including the thickness, which implies that an entire InAs layer is indeed formed through the widening of the InAs traces.

In the case of Figure 3a (where the vertical NW was just starting to form), HRTEM image (Figure 3c) of the interface between Au and InAs confirmed that the base has the ZB structure. Figure 3d is a HRTEM image showing the junction between the base (II) and the InAs trace (I), clearly present the epitaxially grown base on the underlying InAs trace (horizontal stacking faults are occasionally observed). For the developed NWs (as in the case of Figure 3b), HRTEM image (Figure 3e) shows that it has the WZ structure. Moreover, we cannot identify any WZ structure in the bases, suggesting that the base must be formed before the vertical NW growth. The ZB-structured bases were also observed in GaAs and InAs homoepitaxy, which have been ascribed to the low III-group supersaturation of the Au nanoparticle during growth initiation.[15]

In conclusion, the evolution of InAs NWs on the GaAs (111)B substrate was determined by systematic electron microscopy investigations. The interfacial energy between the Au/InAs is higher than that between the Au/GaAs, horizontal InAs traces with the ZB structure form during the initial stage. The catalysts preferentially retain interfaces with GaAs substrate and with InAs {111} planes. As a result, traces form along the ⟨112⟩ directions on the GaAs substrate. Vertical InAs NWs initiate when elongated traces intersect. As a result of the randomly distributed Au catalyst on the GaAs substrate, vertical InAs NWs have uneven heights across the substrate. An extra ZB base forms before the WZ-structured InAs NWs start to form.

Experimental Section

Growth: Semi-insulating GaAs $\{111\}_B$ substrates were functionalized by immersion in 0.1% poly-L-lysine solution spread with

© 2009 Wiley-VCH Verlag GmbH & Co. KGaA, Weinheim

colloid solution containing 30-nm-diameter Au particles. InAs was grown on these substrates by horizontal-flow metal–organic chemical vapor deposition at a pressure of 100 mbar and a total gas flow rate of 15 slm. The substrates were annealed in situ at 600 °C under AsH_3 ambient to desorb surface contaminants. After cooling to 450 °C, trimethylindium was introduced to initiate growth. The nominal V:III ratio was 44. Four samples were prepared with different InAs growth times: 1, 5, 10, and 60 min.

Characterization: The samples were investigated using high-resolution SEM (JEOL JSM890 with a cold field-emission gun) and TEM (FEI Tecnai F20 equipped with EDS for compositional analysis and FEI Tecnai F30). Two aspects of TEM studies were carried out: 1) The structure of individual NWs was studied by ultrasonicating the samples in ethanol for 20 min and dispersing those broken NWs on the holey carbon film; 2) ⟨110⟩ cross-section TEM specimens for understanding the initiation growth of NWs were prepared by cutting, grinding, and polishing, followed by the Ar-ion-beam thinning with an energy of <4 keV, incident beam angles of ±4 degrees, and a beam current of $<3\,\mu A$.

Keywords:
epitaxy · GaAs · InAs · interfacial energy · nanowires

[1] a) T. Martensson, C. P. T. Svensson, B. A. Wacaser, M. W. Larsson, W. Seifert, K. Deppert, A. Gustafsson, L. R. Wallenberg, L. Samuelson, *Nano Lett.* **2004**, *4*, 1987–1990; b) Y. Huang, X. F. Duan, C. M. Lieber, *Small.* **2005**, *1*, 142–147; c) H. J. Fan, P. Werner, M. Zacharias, *Small.* **2006**, *2*, 700–717; d) A. J. Mieszawska, R. Jalilian, G. U. Sumamasekera, F. P. Zamborini, *Small.* **2007**, *3*, 722–756.

[2] R. S. Wagner, W. C. Ellis, *Appl. Phys. Lett.* **1964**, *4*, 89–90.

[3] a) J. Zou, M. Paladugu, H. Wang, G. J. Auchterlonie, Y. N. Guo, Y. Kim, Q. Gao, H. J. Joyce, H. H. Tan, C. Jagadish, *Small* **2007**, *3*, 389–393; b) H. J. Joyce, Q. Gao, H. H. Tan, C. Jagadish, Y. Kim, X. Zhang, Y. N. Guo, J. Zou, *Nano. Lett.* **2007**, *7*, 921–926; c) Y. Kim, H. J. Joyce, Q. Gao, H. H. Tan, C. Jagadish, M. Paladugu, J. Zou, A. A. Suvorova, *Nano Lett.* **2006**, *6*, 599–604.

[4] A. G. Milnes, A. Y. Polyakov, *Mater. Sci. Eng. B* **1993**, *18*, 237–259.

[5] E. Tournie, K. H. Ploog, C. Alibert, *Appl. Phys. Lett.* **1992**, *61*, 2808–2810.

[6] a) X. Z. Liao, J. Zou, X. F. Duan, D. J. H. Cockayne, R. Leon, C. Lobo, *Phys. Rev. B.* **1998**, *58*, R4235–R4237; b) R. Leon, S. Marcinkevičius, X. Z. Liao, J. Zou, D. J. H. Cockayne, S. Fafard, *Phys. Rev. B.* **1999**, *60*, R8517–R8520.

[7] M. T. Bjork, B. J. Ohlsson, T. Sass, A. I. Persson, C. Thelander, M. H. Magnusson, K. Deppert, L. R. Wallenberg, L. Samuelson, *Nano Lett.* **2002**, *2*, 87–89.

[8] a) M. Yazawa, M. Koguchi, K. Hiruma, *Appl. Phys. Lett.* **1991**, *58*, 1080–1082; b) M. Koguchi, H. Kakibayashi, M. Yazawa, K. Hiruma, T. Katsuyama, *Jpn. J. Appl. Phys.* **1992**, *31*, 2061–2065; c) B. J. Ohlsson, M. T. Bjork, A. I. Persson, C. Thelander, L. R. Wallenberg, M. H. Magnusson, K. Deppert, L. Samuelson, *Physica E.* **2002**, *13*, 1126–1130; d) L. E. Jensen, M. T. Bjork, S. Jeppesen, A. I. Persson, B. J. Ohlsson, L. Samuelson, *Nano. Lett.* **2004**, *4*, 1961–1964; e) H. D. Park, S. M. Prokes, R. C. Cammarata, *Appl. Phys. Lett.* **2005**, *87*, 063110(3).

[9] L. E. Jensen, M. T. Bjork, S. Jeppesen, A. I. Persson, B. J. Ohlsson, L. Samuelson, *Nano. Lett.* **2004**, *5*, 761–764.

[10] K. A. Dick, Z. Geretovszky, A. Mikkelsen, L. S. Karlsson, E. Lundgren, J.-O. Malm, J. N. Andersen, L. Samuelson, W. Seifert, B. A. Wacaser, K. Deppert, *Nanotechnology.* **2006**, *17*, 1344–1350.

[11] M. He, M. M. E. Fahmi, S. N. Mohammad, R. N. Jacobs, L. Salamanca-Riba, F. Felt, M. Jah, A. Sharma, D. Lakins, *Appl. Phys. Lett.* **2003**, *82*, 3749–3751.

[12] C. Y. Zhi, X. D. Bai, E. G. Wang, *Appl. Phys. Lett.* **2004**, *85*, 1802–1804.

[13] M. Paladugu, J. Zou, Y. N. Guo, G. J. Auchterlonie, H. J. Joyce, Q. Gao, H. H. Tan, C. Jagadish, Y. Kim, *Small* **2007**, *3*, 1873–1877.

[14] M. Paladugu, J. Zou, G. J. Auchterlonie, Y. N. Guo, Y. Kim, H. J. Joyce, Q. Gao, H. H. Tan, C. Jagadish, *Appl. Phys. Lett.* **2007**, *91*, 133115.

[15] a) F. Glas, J.-C. Harmand, G. Patriarche, *Phys. Rev. Lett.* **2007**, *99*, 146101(4); b) K. A. Dick, K. Deppert, T. Marensson, B. Mandl, L. Samuelson, W. Seifert, *Nano. Lett.* **2005**, *5*, 761–764.

Received: May 14, 2008
Revised: September 2, 2008
Published online: January 16, 2009

© 2009 Wiley-VCH Verlag GmbH & Co. KGaA, Weinheim